Carbonation and related behaviors of hardened cement pastes under different hydration degrees

Xu, Yaowen; Liang, Xuhui; Wan, Chaojun; Yang, Hongyu; Feng, Xiaming

DOI
10.1016/j.cemconcomp.2023.105079

Publication date
2023

Document Version
Final published version

Published in
Cement and Concrete Composites

Cement and Concrete Composites 140 (2023) 105079

Contents lists available at ScienceDirect

Cement and Concrete Composites

journal homepage: www.elsevier.com/locate/cemconcomp

Carbonation and related behaviors of hardened cement pastes under different hydration degrees

Yaowen Xu [a,b], Xuhui Liang [c], Chaojun Wan [a,b,*], Hongyu Yang [a], Xiaming Feng [a]

[a] College of Materials Science and Engineering, Chongqing University, Chongqing, 400045, PR China
[b] Chongqing International Joint R&D Centre of Low Carbon and High Performance Cement-Based Materials, Chongqing, 400044, PR China
[c] Department of Materials, Mechanics, Management & Design, Faculty of Civil Engineering and Geoscience, Delft University of Technology, Delft, the Netherlands

ARTICLE INFO

Keywords:
Cement paste
Carbonation
Mineral composition
Water content
Drying shrinkage

ABSTRACT

This paper develops a kind of molded disc samples to investigate the carbonation and related behaviors of hardened cement pastes under different previous hydration degrees. Weight and length changes of cement pastes over time are monitored during a multistep process including carbonation, drying, rewetting, and redrying. The combination of X-ray diffraction (XRD) and thermogravimetric analysis (TGA) is used to identify and quantify the mineral compositions of carbonated cement pastes. An exponential function between CO_2 uptake capacity and hydration time of cement pastes is established, which shows that the CO_2 uptake capacity of cement pastes decreases dramatically at the very beginning days of hydration and then remaining relatively stable as hydration time is prolonged. Two reasons for this finding are revealed: i) the equilibrium between the carbonation and the post-carbonation reaction of carbonation product, i.e., silica-alumina gel; ii) refining of pore structures by hydration products which hinders carbonation. A clearer zonation of carbonation areas is proposed, and the spatial distribution equations of CO_2 absorption are initially established. By monitoring carbonation and drying behavior of cement pastes with different hydration ages, it is revealed that carbonation reduces drying shrinkage of cement pastes especially for early-age samples, whereas drying increases carbonation shrinkage. By investigating the water changes during the multistep process, it is found that water is little released during the carbonation of C–S–H gels. New insight into mechanism of carbonation shrinkage is provided by a newly proposed model.

1. Introduction

Carbonation in cement-based materials involves outside gaseous CO_2 diffusing into solid mass, and a series of chemical reactions, in which not only hydration products, but also unhydrated clinker minerals can participate in [1,2]. As a consequence, carbonation reactants change with carbonation starting time, i.e., the hydration time of cement pastes. This causes dynamical and uncertain changes in chemical (e.g., CO_2-uptake rate and capacity) and physical (e.g., water content and carbonation deformation) properties, as well as post-carbonation properties (e.g., strength and drying shrinkage). Actually, the effects of carbonation on the compositions, structures, and properties of cement-based materials, as well as the improvement of the carbonation process are widely investigated [3–12]. Due to the emphasis on consuming greenhouse gas CO_2 by carbonation [10,13,14], scientists try to develop the potential utilization of concrete for carbon capture and sequestration (CCS) [15,16]. Despite lots of progress, the understanding on carbonation of hardened cement pastes under different hydration degrees is still needed.

In most traditional cases, more mature samples, for example, concrete with a hydration age of 28 d or longer, is employed for carbonation investigation [4,7,17–20]. However, this simplification ignores the effect of hydration time on carbonation, accordingly, inescapably causes the lack of understanding on the carbonation of concrete with shorter hydration time. Therefore, it is worth studying the carbonation of cement pastes with a broader range of hydration degrees, especially covering the lower hydration degree, to get a full understanding of the effect of hydration on carbonation.

There exists the effect of hydration degree on carbonation even in the same concrete sample. For example, as a result of the diffusion of CO_2 from the surface to the inside of the sample, the inside will be carbonated later and possibly has a greater hydration degree at the starting

* Corresponding author. College of Materials Science and Engineering, Chongqing University, Chongqing, 400045, PR China.
E-mail address: cjwan@cqu.edu.cn (C. Wan).

https://doi.org/10.1016/j.cemconcomp.2023.105079
Received 8 January 2023; Received in revised form 27 March 2023; Accepted 13 April 2023
Available online 5 May 2023

time of carbonation compared with the surface. However, as carbonation is a water-demanding process [5,21], it is inapplicable to arrest the hydration of cement pastes to ensure samples with the same maturity for the carbonation at a specific hydration degree. For the purpose of studying the carbonation behavior of early-hydration-age cement pastes, CO_2 diffusion should be neglected.

On the other hand, concrete is heterogeneous, with multiple composites and pore structures. This makes the CO_2 diffusion as well as the reaction process heterogeneous and influenced by multiple factors. It is suggested that in order to simplify the study on carbonation, the CO_2 diffusion should be skillfully neglected.

To neglect the diffusion process, one dimension of the sample could be much smaller than the other two dimensions. The disc sample meets this requirement, and has been chosen in the study of drying shrinkage of cement pastes [22]. Commonly, the discs are cut from cylindrical samples using a water-lubricated diamond saw [23]. However, during cutting, the lubricant, for example, water, can lead to the mass loss especially the loss of $Ca(OH)_2$ of samples. The interchanges of phases are inevitable, even if the $Ca(OH)_2$ saturated solution is used as the lubricant. This mass loss may have little influence on drying shrinkage, however, it certainly affects carbonation of cement pastes as $Ca(OH)_2$ is one of the main reactants of carbonation. Furthermore, micro-cracks may be induced during cutting, which also have effects on the carbonation process. Therefore, it is necessary to mold disc samples directly for this study, which can provide gradient-free carbonation, that is, the CO_2 diffusion is skillfully neglected.

Carbonation-induced crack is regarded important for the durability, so widely considered by previous studies [6,19,24,25]. The carbonation deformation of cement pastes should be correlated with the cement hydration degrees. The changes of carbonation reactants and the changes of rigidity with hydration would result in the varied carbonation deformation. This process can be monitored by measuring the diameter of disc sample. Moreover, gradient-free disc samples could reflect more authentic deformation than bulk samples as the carbonation of the latter is not uniform from surface to inside.

Carbonation causes deformation, and may affect other kinds of deformations, for instance, drying shrinkage. Carbonation can generate water [2,18] and change the pore structures of concrete [26–28]. These two changes are closely related to the drying shrinkage behavior, which can also be investigated by using disc samples.

In this paper, a disc mold is designed to shape disc samples. Using the disc samples, the carbonation and related behaviors of cement pastes under different hydration degrees are carefully investigated, which gives a better understanding on and deeper insight into the carbonation reaction, carbonation shrinkage, and post-carbonation drying shrinkage of cement pastes.

2. Materials and methods

2.1. Materials and mix proportion

P·I 42.5 cement (stated in Appendix A of Chinese standard GB 8076 Concrete Admixtures [29], composed of at least 95% clinker and minor additional constituents, similar to European CEM I) and distilled water are employed to prepare cement paste. The chemical composition of P·I 42.5 cement is tested by the manufacturer and calculated through Bogue equations, as listed in Table 1. CO_2 gas with a purity of 99.5% is used for carbonation. N_2 gas with a purity of 99.99% is used to provide an inert atmosphere upon carbonation for reference samples as well as samples with CO_2-free drying.

Mix proportion: the water-to-cement ratio of cement paste adopted in this study is 0.5.

Table 1
Chemical analysis of P·I 42.5 cement and its corresponding clinker minerals calculated by Bogue equations.

Chemical composition	Content (wt. %)	Clinker mineral	Content (wt. %)
SiO_2	20.08	C_3S	59.38
Al_2O_3	5.09	C_2S	15.59
Fe_2O_3	3.81	C_3A	7.28
CaO	63.41	C_4AF	11.64
MgO	2.06		
SO_3	2.33		
Na_2Oeq	0.55		
f-CaO	0.88		
Cl^-	0.016		
LoI	1.72		

2.2. Methods

2.2.1. Disc molding

In order to mold the disc cement paste sample, a special mold is designed as shown in Fig. 1. The mold is divided into three functional parts to make it both mold and demold easily. Using the mold, disc samples with a diameter of 25 mm and thickness of 1 mm are shaped and demolded after 24 h. The demolded samples are sealed with polythene films until the testing ages.

2.2.2. Reaction device

To supply CO_2 and moisture for carbonation, a reaction device is designed as shown in Fig. 2. The device is a 180 ml bottle with cover. At the bottom of the bottle, about 30 ml of distilled water is previously introduced inside to provide a high enough relative humidity (RH) environment and to avoid any drying caused by lower RH during carbonation. A grid plate is placed in the middle of the bottle to hold the disc sample. The other part of the bottle is filled with CO_2 for carbonation under atmospheric pressure (not specially controlled but very similar) or N_2 for carbonation free as the reference. The volume of the device is specially designed more than enough according to the maximum CO_2 absorption of samples to ensure the amount of CO_2 is sufficient in the whole period of the reaction even without replenishment, although gases are replenished after each measurement of samples. The device can create a separate environment for each disc, ensuring that the testing of one sample does not have any effect on the others.

2.2.3. Experimental methods

Disc samples with previous hydration ages of 1 d, 3 d, 7 d, 14 d, 28 d, 60 d, 180 d, and 360 d are subject to five successive processes, i.e., carbonation (the most important reaction of this study, at 20 °C), drying (detailedly study the water changes and drying shrinkage, including drying at 20 °C and at 50 °C), rewetting (clarify the water changes and statuses, at 20 °C), and redrying (judge whether continuous hydration happens or not, and bridge the results between the measurement here and the following TGA test, etc., at 50 °C) to investigate their carbonation and related behaviors under different hydration degrees. 50 °C is chosen for drying and redrying for the reason that at this temperature, disc samples can be dried quickly without hydration products being destroyed [30]. The experiment process is schematically detailed as shown in Fig. 3. During the whole experimental process, samples are weighed by an analytical balance and gaged lengths by a micrometer at certain times. Three lines are slightly drawn and numbered accordingly on each disc before carbonation to monitor length changes, as shown in Fig. 3. The mean value of the length changes is regarded as the length change of samples. The temperature in the laboratory is controlled at 20 °C ± 1 °C by an air conditioner.

Firstly, the initial weight and lengths of each sample are measured. Then each sample is put into one separate reaction device and the reaction device is filled with CO_2 to initiate carbonation or N_2 for

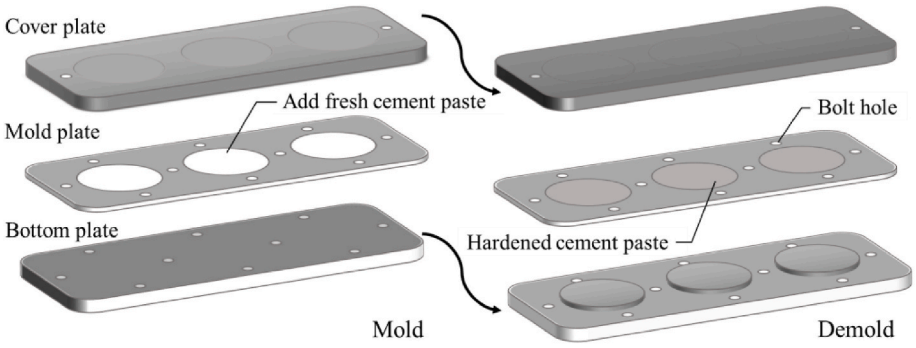

Fig. 1. Diagram of the purpose-built mold for preparing disc samples.

Fig. 2. Schematic diagram of the reaction device for carbonation (CO_2) or carbonation free (N_2) as the reference.

reference. The gas filling process is from the bottom to the top of the device and kept for more than 10 s to ensure all the air in device is fully removed by this kind of replacement. Afterwards, the device is covered immediately to avoid gas leaking. At the reaction time of 10 min, 30 min, 1 h, 5 h, 10 h, 24 h, and then every 24 h, the sample is taken out to be weighed, gaged lengths to trace the carbonation process. The measurement process takes about 1–2 min every time. After each measurement, the sample is put back and the bottle is replenished with CO_2 or N_2. The equilibrium of weight and length is considered the stoppage of carbonation under the reaction conditions [21]. Note whether the carbonation has completed should be further verified according to the amount of residual reactants and products. After reaching equilibrium, every sample is transferred into another bottle without water for a following drying to investigate the subsequent drying behavior under laboratory temperature. The weight and length of samples are tested at 0 h, 1 h, 5 h, 10 h, 24 h, and then every 24 h until equilibrium. After finishing the drying under laboratory temperature, the bottle together with sample is put into an oven to dry under 50 °C and tested every 24 h until equilibrium to quantify the change of water content. After oven drying, the samples are rewetted under laboratory temperature and redried under 50 °C. During every stage of drying, rewetting, and redrying, N_2 is supplied for drying and preventing carbonation by CO_2 in air.

The carbonated groups are named group C. Non-carbonated groups are set for comparison and named group N. Given that samples may release or absorb water during the reaction process as a result of humidity equilibrium, the weight changes of group C are subtracted by the weight changes of group N (named C–N) to approximately eliminate the effect that is not induced by carbonation. It should be noted that actually the water changes of group C induced by humidity equilibrium is not the same as those of group N.

To identify the mineral compositions of samples with or without carbonation, the redried samples are ground into powders and measured by X-ray powder diffractometer (Panalytical B·V., PfANalytical X'Per Powder) with Cu Kα radiation at 40 kV and 40 mA. The measuring range of 2θ is 5–60°with a total scanning time of 10 min.

To quantify $Ca(OH)_2$, $CaCO_3$, and bound water, the redried powdered samples are measured by Thermogravimetric analyzer (Mettler Toledo, TGA2) under N_2 atmosphere (50 ml/min) from 30 °C to 1100 °C, with the heating rate of 10 °C/min. The quantification of the amounts of $Ca(OH)_2$ and $CaCO_3$ is performed using the tangential method [30]. The bound water is calculated by subtracting the mass loss of $CaCO_3$ decomposition from the mass loss between 105 °C and 1100 °C.

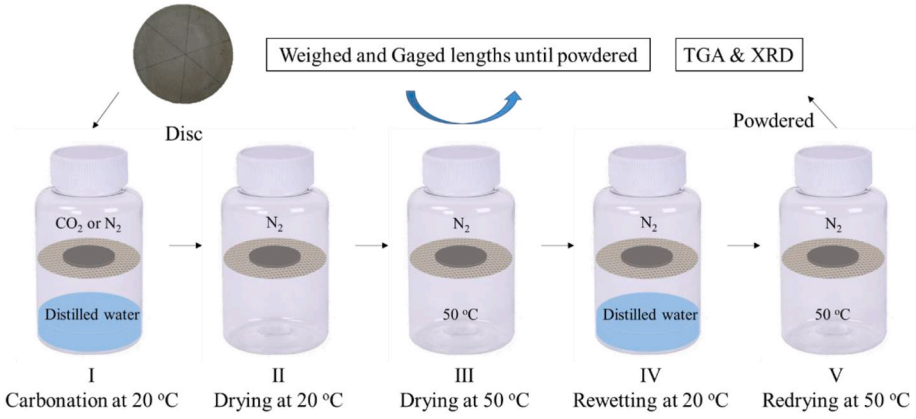

Fig. 3. Experiment process of carbonation, drying, rewetting, and redrying.

3. Results and discussion

3.1. CO_2 uptake capacity

It is important to know the CO_2 uptake capacity of cement pastes, i.e., how much CO_2 can be absorbed by cement pastes, for the calculation of carbon footprint as well as the study of carbonation. The CO_2 uptake capacity of cement paste may be affected by its hydration degrees. To investigate the effect of hydration on the CO_2 uptake capacity of cement paste, disc samples at hydration ages of 1 d, 3 d, 7 d, 14 d, 28 d, 60 d, 180 d, and 360 d are carbonated. The weights of samples are measured during carbonation until constant weights are reached. The corresponding weight changes of the constant weights are named the ultimate weight changes, which reflects the CO_2 uptake capacity of samples. Fig. 4 shows the carbonation-induced ultimate weight changes (C–N) of samples as a function of hydration time.

It can be seen from Fig. 4 that with the increase of hydration time, the ultimate weight changes induced by carbonation decrease dramatically when the hydration time is short enough, and then remain relatively constant after 28 d. This notable result indicates that cement pastes with different hydration degrees have different CO_2 uptake capacities. The differences in CO_2 uptake capacities may be the result of the changes in carbonation reactants or/and the changes in compactability of microstructures induced by hydration. As mentioned above, both clinker minerals and their hydration products can be carbonated. With hydration going on, the amounts of hydration products increase while those of clinker minerals decrease. The decreased CO_2 uptake capacities with hydration at early ages means that in the cement paste, carbonation of hydration products at this moment is difficult or the carbonation of residual carbonatable substances is inhibited by the dense layer of hydration or carbonation products. The reason can be speculated as follows. $CaCO_3$ and substances with very low Ca/Si, i.e., silica-alumina gel are generated through carbonation reaction [31,32]. One of the carbonation products, silica-alumina gel, is found to be a pozzolanic material with much higher specific surface area than the metakaolin and silica fume and therefore high reactivity [33]. The highly reactive silica-alumina gel can generate C–S–H gels in the presence of $Ca(OH)_2$. If the hydration is called the first or primary reaction, the carbonation is called the second or secondary reaction, this kind of post-carbonation reaction of carbonation products could be named the third or tertiary reaction. This third reaction can alter the carbonation product into new carbonation reactant. Hence, there could be a dynamic equilibrium between the carbonation and the third reaction. The equilibrium tends to the later when the hydration time is prolonged and $Ca(OH)_2$ increases.

According to the speculation, two substances, $Ca(OH)_2$ and water, are required to maintain the equilibrium between the carbonation and the third reaction. If free water is limited, the equilibrium would be broken, consequently, CO_2 uptake capacity would increase. To verify this, disc samples with a hydration age of 28 d are dried at 50 °C for 5 days to release most of the free water without destroying hydration products [30], and then carbonated in a 99.5% CO_2 atmosphere at 20 °C without supplying water at the bottom of the bottle (named C (28 d-dried)). A blank experiment is conducted simultaneously by placing the dried samples in a N_2 atmosphere (named N (28 d-dried)). The weight changes and length changes (discussed later) of these experiments and their difference are shown in Fig. 5. It can be seen from Fig. 5 (a) that only a small amount of CO_2 is absorbed in the first few days of reaction time, which is very different from the carbonation with sufficient moisture supplied (discussed later in 3.2). This is because carbonation needs water to dissolve reactants, including CO_2 and Ca-bearing phases. As samples slowly absorbing water from atmosphere during the short-tested time, carbonation is reinitiated and a large amount of CO_2 is absorbed. Compared with the initial weight before drying, carbonation-induced weight change is about 11.50%. This value is higher than that of the sample at the same hydration age and carbonated with enough water provided (2.72%). The result indicates that as the third reaction is hindered, CO_2 uptake capacity increases.

However, the carbonation-induced weight change of the 50 °C-dried-sample at 28 d is still lower than that of the sample carbonated at 1 d (14.07%). Moreover, it is noticed that hydration becomes relatively stable after 200 d [34], while CO_2 uptake capacities keep relatively constant after 28 d. These mean in addition to the equilibrium between the carbonation and the third reaction, there exists another reason causing the difference in CO_2 uptake capacity. As hydration time is prolonged, the microstructure is refined by hydration products, which makes the contact between carbonation reactants more and more difficult, hence the carbonation is hindered. Therefore, the decrease of CO_2 uptake capacities with hydration ages attributes to the changes of both compositions and microstructures.

As shown in Fig. 4, the relationship between CO_2 uptake capacities and hydration time fits well as an exponential function, with R^2 more than 0.98. This relationship is conducive to our understanding of carbonation area zonations and will be discussed in 3.3.

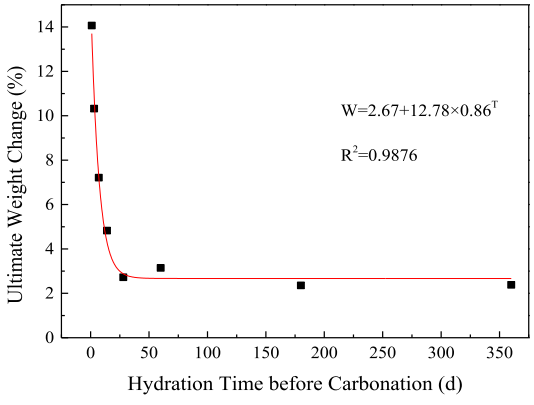

Fig. 4. Carbonation-induced ultimate weight changes of samples as a function of hydration time.

3.2. Carbonation process

Carbonation of cement pastes is considered to be controlled by the diffusion of CO_2, dissolution of carbonation reactants, and precipitation of carbonation products [4,14,24,35]. In gradient-free circumstances, diffusion could be neglectable. With sufficient CO_2 and moisture supplied, the dissolution of reactants is fast enough, and can also be neglected. Therefore, the precipitation of the carbonation products, including nucleation and growth, becomes the main control process in our thin disc experiments. Nucleation and growth follow an exponential relationship with time according to the Avrami or JMAK equation [36–38] (Eq. (1)),

$$X(t) = 1 - \exp\left[-(kt)^m\right] \quad (1)$$

where X(t) represents the volume fraction that has transformed at time t, k is the rate constant, and m refers to the Avrami index.

To demonstrate the carbonation process of cement pastes, the carbonation-induced weight changes of 1 d and 28 d samples as a function of carbonation time are recorded and shown in Fig. 6. It is obviously shown that carbonation occurs at a beginning with fast rate before equilibrium. The weight changes of 90% to equilibriums can be reached within 1 d. The reaction goes to equilibrium in the experimental conditions around 4 d. Even though there is difference between the ultimate weight changes of two curves, the relationships between weight changes and carbonation time of both curves fit well as an exponential function, with R^2 more than 0.90.

According to the relationships shown in Fig. 6, the Avrami index is 1,

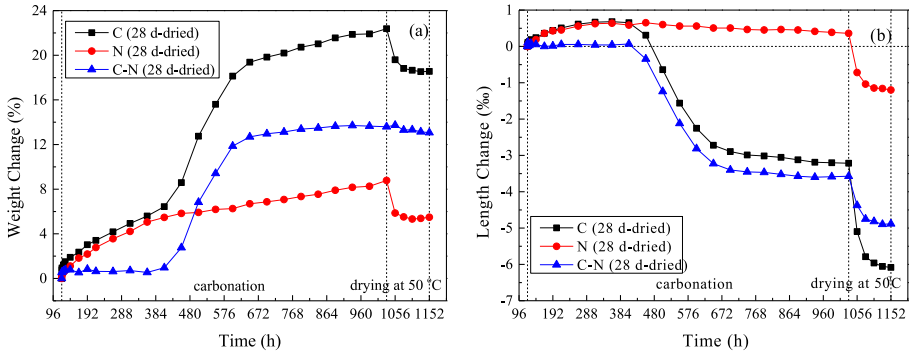

Fig. 5. (a) Weight change and (b) length change of disc samples carbonated after 5 days of 50 °C-drying treated at hydration age of 28 d.

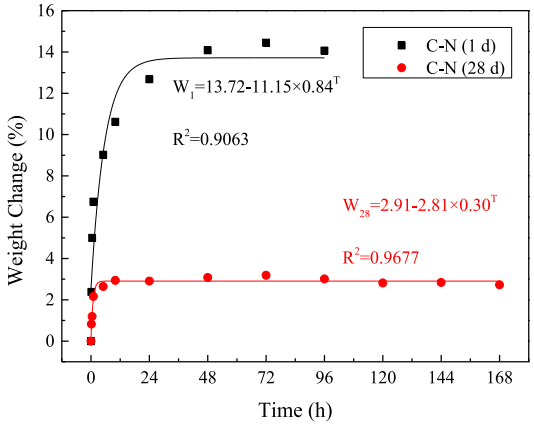

Fig. 6. Weight changes of samples carbonated at hydration age of 1 d and 28 d as a function of carbonation time.

which means calcium carbonate precipitates via heterogeneous nucleation and one-dimensional growth. This is considered as the reason that $CaCO_3$ crystal usually grows on the surface of hydration products and aggregates [18] with small size [39].

3.3. Carbonation area zonation with CO_2 uptake

The zonation of the carbonation areas is important, as it can reveal the carbonation process of concrete and guide engineering practices. In practice, pH indicator such as phenolphthalein is normally used to determine the carbonation depth of concrete. The pink part is regarded as the non-carbonated zone while the colorless part is considered to be carbonated. This method is convenient and practical from an engineering point of view, however, it is rough from a scientific perspective. As we know, the pH of cement paste is usually higher than 12.5 [40]. Phenolphthalein shows a color change in the pH range of 8.2–9.8 [5]. Therefore, the color changes are not always coincident with carbonation. Moreover, it is believed that there is a semi (partial)-carbonation zone between the complete (full) carbonation zone and non-carbonation zone [41]. The corrosion of steel bar may also take place in the partial-carbonation zone, whereas this zone cannot be indicated by using phenolphthalein. In addition, the division stated in Ref. [41] regards the full carbonation zone as a uniform part, with phases remaining consistent throughout. However, this is not the case for samples carbonated at early hydration ages as discussed in 3.1 and 3.2. There should be distinctions between early-age carbonated parts and mature-age carbonated parts as they have different CO_2 uptake capacities. These differences will not disappear with the elapse of carbonation time.

The CO_2 uptake capacity discussed in 3.1 could reflect the ultimate state of carbonated cement paste, which can be used to understand the carbonated zone. The carbonation process discussed in 3.2 can be used to comprehend the partially-carbonated zone where the carbonation is still in progress. For carbonation investigation, samples of cement-based materials can be cut layer by layer to analyze compositions and properties of part with different depth [5,18], vice versa, stacking piece samples together could also be used to reflect carbonation behaviors. As the carbonation investigated in this study is almost gradient free, a link should be built to transfer the gradient-free carbonation to gradient carbonation. This link would be the equation of CO_2 diffusion.

The relationship between CO_2 diffusion and time is shown as Eq. (2) [42],

$$X = K\sqrt{t} \tag{2}$$

where X represents the carbonation depth, K refers to the carbonation coefficient, and t is carbonation time. Suppose the carbonation of cement paste has no impact on the hydration of non-carbonated part. The relationship between weight changes and time can be translated, according to Eq. (2), into the relationship between weight changes and depths, as depicted in Fig. 7. As shown in Fig. 7, the carbonation zone is divided into 3 parts, namely carbonated zone, partially-carbonated zone, and non-carbonated zone. In different zones, the generated $CaCO_3$ after carbonation of the early-hydration-age cement paste is illustrated in Fig. 8. The three zones can be further subdivided into 5 parts (shown in Fig. 9) and described as follows.

Carbonated zone: This zone is subdivided into full carbonation zone and carbonation stopped zone. The full carbonation zone is where the

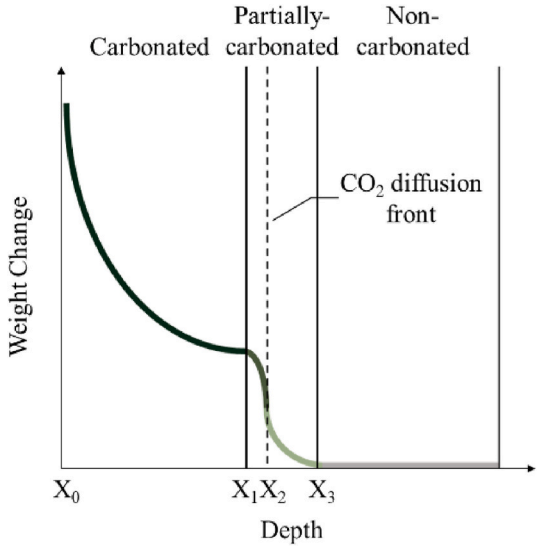

Fig. 7. Illustration of weight change induced by carbonation along depth.

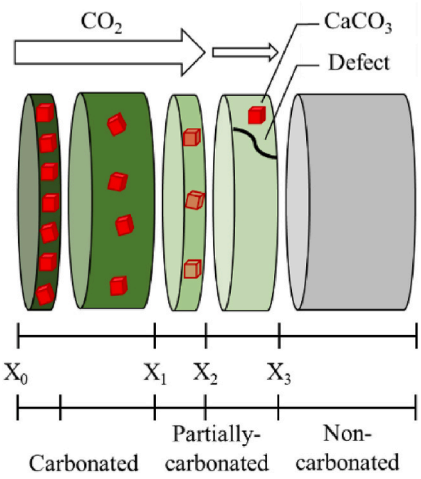

Fig. 8. Illustration of the generated $CaCO_3$ along different zones after carbonation of the early-hydration-age cement paste.

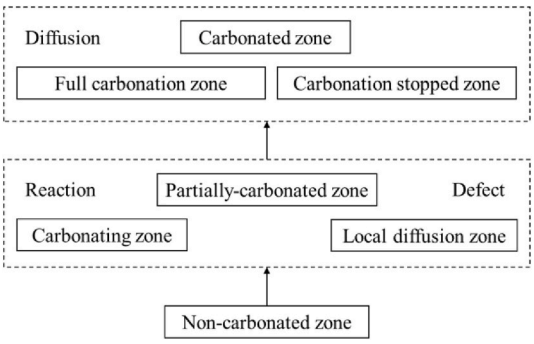

Fig. 9. Subzonations of carbonation zone.

carbonatable phases are all carbonated. The carbonation stopped zone is where carbonation is stopped because of 2 reasons, i.e., i) the equilibrium between the carbonation and the third reaction; ii) the limited contact of carbonation reactants with CO_2 as microstructure refined. Although there are carbonatable phases in carbonation stopped zone, carbonation cannot proceed in constant reaction conditions. The carbonated zone is mainly controlled by diffusion [14].

Partially-carbonated zone: This zone is subdivided into carbonating zone and local diffusion zone. The carbonating zone is where CO_2 has accessed and the reactions are proceeding. The local diffusion zone is where CO_2 has locally diffused as cement pastes are heterogeneous and have defects such as (micro-) cracks and air voids, which makes carbonation in local diffusion zone proceeds preferentially. Partially-carbonated zone is mainly controlled by reaction and defect, and is dependent on the cement type and water-to-cement ratio. Partially-carbonated zone will evolve into carbonated zone and keep going forward with time.

Non-carbonated zone: This zone is where carbonation has not started. With time going on, non-carbonated zone will turn into partially-carbonated zone and then carbonated zone.

According to the description above, we can initially establish the spatial distribution equations of CO_2 absorption, shown as Eq. (3),

$$\frac{dm_{CO_2}}{dx} = \begin{cases} C_u + H \bullet \gamma_H{}^{x^2/K^2}, & 0 \le x \le x_1 \\ C_u - C_s \bullet \gamma_C{}^{(x_2-x)^2/K^2}, & x_1 < x < x_2 \\ C_\varnothing \bullet \gamma_\varnothing{}^{(x-x_2)^2/K_\varnothing{}^2}, & x_2 \le x \le x_3 \\ 0, & x > x_3 \end{cases} \quad (3)$$

where x_1, x_2, x_3, are the front of carbonated zone, the front of carbonating zone (i.e. the front of CO_2 diffusion), and the front of local diffusion zone (i.e. the front of partially-carbonated zone), respectively. C_u is CO_2 uptake capacity of mature cement paste. C_s is a parameter related to carbonation speed. H refers to the influence of hydration on CO_2 uptake capacities. γ_H, γ_C, and γ_Φ are parameters related to hydration, carbonation and defect, respectively. K, K_Φ refer the diffusion coefficients of CO_2 in cement paste and defect, respectively. It is noticeable that this equation describes the carbonation starts at early hydration age such as early at demold time. The parameters and applicability of Eq. (3) to other conditions, e.g., lower CO_2 concentration are still to be further studied.

This carbonation division reminds us carbonation is a very complex process. There are different states even in carbonated zone. The concrete with hydration age of 28 d is usually used to judge carbonation property according to engineering standards [43,44]. However, carbonation starts earlier than 28 d in practice. Therefore, the effect of carbonation may be underestimated. Carbonation needs to be further and deeply investigated.

3.4. Drying shrinkage of carbonated cement pastes

It has been verified that cement pastes with different hydration ages have different CO_2 uptake capacities. This difference may induce consequent influences on the properties of carbonated cement pastes. Carbonation causes a process of absorbing a new substance, i.e. CO_2, into cement pastes, as a result, alters the pore structures of cement pastes [45,46]. Pore structures are associated with the drying shrinkage behavior [47]. Therefore, the drying and rewetting behaviors of carbonated disc samples are investigated.

Fig. 10 shows the weight and length changes of 1 d and 28 d disc samples throughout the experimental process of 5 stages including carbonation, drying at 20 °C, drying at 50 °C, rewetting, and redrying at 50 °C as marked in Fig. 3. As shown in Fig. 10(a), the weights of 1 d samples under N_2 atmosphere decrease at first then increase for the first 96 h. The decrease of weights attributes to the water release caused by the blowing of N_2 gas, and the increase of weights is attributed to moisture equilibrium between samples and environment. By contrast, the weights of samples of group N treated at hydration time of 28 d increase for the first 168 h (Fig. 10(e)), which is attributed to the absorption of moisture from the environment as the relative humidity of samples decreases with hydration progressing. These water release or absorption phenomena could also be reasonably believed to occur in carbonation groups, although group C shows continuously increased weight changes during the carbonation stage because the weight increase caused by absorption of CO_2 is more than and offset the weight decrease caused by the possible release of water.

As shown in Fig. 10(c) and (d), for samples carbonated at the hydration time of 1 d, weight changes, as well as length changes of group C are smaller than those of group N during drying process. After drying and rewetting, the lengths of both group C and group N cannot fully recover, indicating that microstructures collapse during the drying process. For group N, the remained weights as well as the diminution of lengths after the second 50 °C drying are higher than those after the first 50 °C drying. This means group N has continued hydration during rewetting. On the contrary, group C has limited continued hydration during rewetting. This phenomenon may be caused by two reasons: unhydrated clinker minerals have been consumed during carbonation stage or continued hydration of clinker minerals is hindered by the dense layer formed by carbonation products. The XRD results presented later verified the possibility of the former.

To identify the mineral compositions of each group, samples C1-1, N1-1, C28–1, N28-1, as well as C (28 d-dried) and N (28 d-dried) are characterized using XRD and the results are shown in Fig. 11. As shown in Fig. 11, there is no $Ca(OH)_2$ in group C carbonated at 1 d. However, Ca

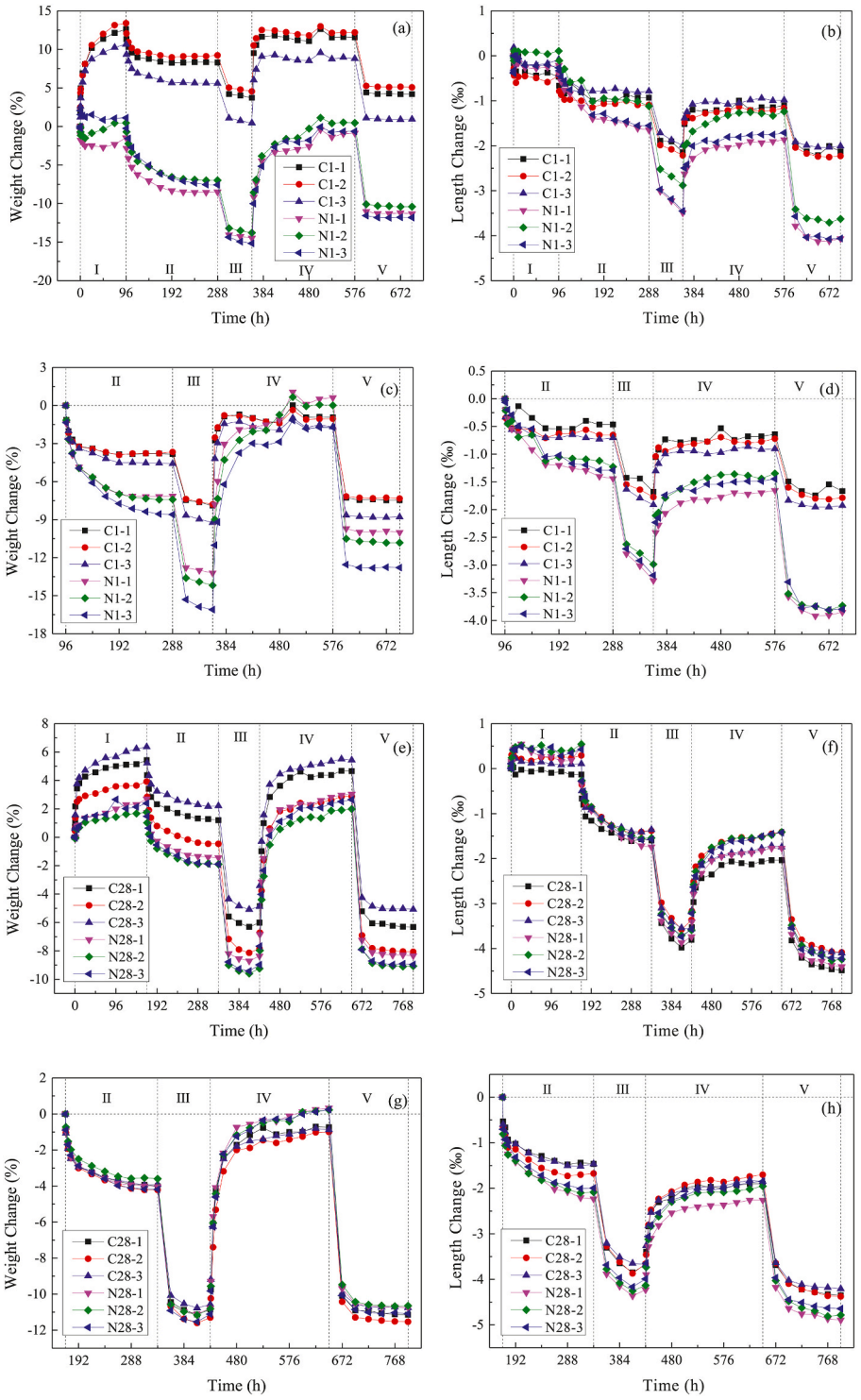

Fig. 10. Weight and length changes of disc samples carbonated at hydration time of 1 d and 28 d during the whole and parts of 5 stages of experimental process. (a)–(d): 1 d; (e)–(h):28 d. (a), (c), (e), and (g): weight changes; (b), (d), (f), and (h): length changes. (a), (b), (e), and (f): start at carbonation stage; (c), (d), (g), and (h): start at drying stage.

$(OH)_2$ does exist in group C carbonated at 28 d. The presence of $Ca(OH)_2$ is the essential requirement of the existence of the equilibrium between the carbonation and the third reaction. There is almost no C_3S or C_2S in group C carbonated at 1 d, which means carbonation obviously consumed the clinker minerals. This agrees with the analyses in previous paragraph about the results of weight and length changes. All of the samples have calcite even for those under the protection of N_2. This possibly indicates that carbonation occurs during the very short time of measuring weight and lengths. Carbonation occurs so fast and ubiquitously wherever there is air. In addition to calcite, aragonite is detected in samples carbonated at 1 d, while vaterite is detected in samples carbonated at 28 d. Both of the metastable forms of calcium carbonate, i.e. aragonite and vaterite, are detected in group C (28 d-dried).

To quantify the amount of CO_2 absorption, samples of each group (i.e. C1-1, N1-1, C28–1, N28-1, as well as C (28 d-dried) and N (28 d-dried)) are tested by TGA and the results are shown in Fig. 12. The

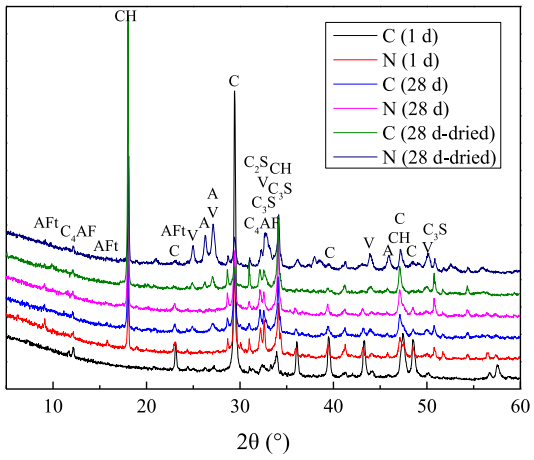

Fig. 11. XRD patterns of samples carbonated at hydration time of 1 d, 28 d, and samples carbonated after 5 days of 50 °C-drying at hydration age of 28 d. C, A, and V refer to calcite, aragonite, and vaterite, respectively.

calculated results from Fig. 12 are listed in Table 2. According to the measured weight changes (Fig. 10(a)) and the amount of CO_2 absorption shown in Table 2, the water loss of group C1-1 after carbonation process is about 10.93%, which is 3.76% higher than that of group N1-1. However, the corresponding length diminution of group C is only slightly bigger than that of group N. For samples carbonated at the hydration time of 1 d, the drying shrinkage is smaller than the reference, and the water loss induced shrinkage during carbonation is also small. Therefore, it is concluded that for the early-age cement pastes, carbonation can reduce drying shrinkage.

It is notable that the peak temperatures of calcium carbonate of different groups are not coincident with each other as shown in Fig. 12. The higher decomposition temperature means the better thermostability. Samples carbonated at 1 d can generate more stable calcium carbonate than carbonation at 28 d. Carbonation in drying condition (group C (28 d-dried)) would also produce more stable calcium carbonate than in wetting condition (group C (28 d)). It is interesting to find in Fig. 12(c) that $Ca(OH)_2$ peak temperature in group C of 28 d is slightly lower than those in group N of 1 d, 28 d, and 28 d-dried. However, group C of 28 d-dried has the highest $Ca(OH)_2$ peak temperature among all groups. It shows the residual $Ca(OH)_2$ of carbonated sample may have differences compared with the generated $Ca(OH)_2$ from hydration. This phenomenon may be related to the carbonation occurring in the interlayer of C–S–H gels, which will be discussed in 3.6.

For samples carbonated at the hydration time of 28 d, weight changes and length changes of group C are very close to those of group N during drying process as shown in Fig. 10(g) and (h). For better comparison, the weight changes and length changes of group N are subtracted from group C, and the results are shown in Fig. 13. As shown in Fig. 13, the influence of carbonation starts at 1 d on drying and drying shrinkage behaviors are much obvious than that starts at 28 d.

3.5. Water changes in carbonation

The presence of water, including free water and bound water, has significant effect on performances of cement pastes. Carbonation needs water to dissolve reactants [5], and water can be generated from carbonation. In addition, changes of pore structure induced by carbonation can also affect the existence of free water [20]. Therefore, the study on water content, water type and its energy state (simply called

Table 2
Calculated results from TGA. (Unit: g/g cement of 1100 °C).

	H_2O of $Ca(OH)_2$[a]	CO_2 of $CaCO_3$[a]	Bound Water[b]
C1	–	0.33118	0.10504
N1	0.01998	0.08180	0.13492
C28	0.02006	0.11323	0.16651
N28	0.03095	0.06299	0.18224
C28-dried	0.01496	0.26159	0.14894
N28-dried	0.03622	0.08387	0.17660

[a] Using the tangential method [30].
[b] Subtracting the mass loss of $CaCO_3$ decomposition from the mass loss between 105 °C and 1100 °C.

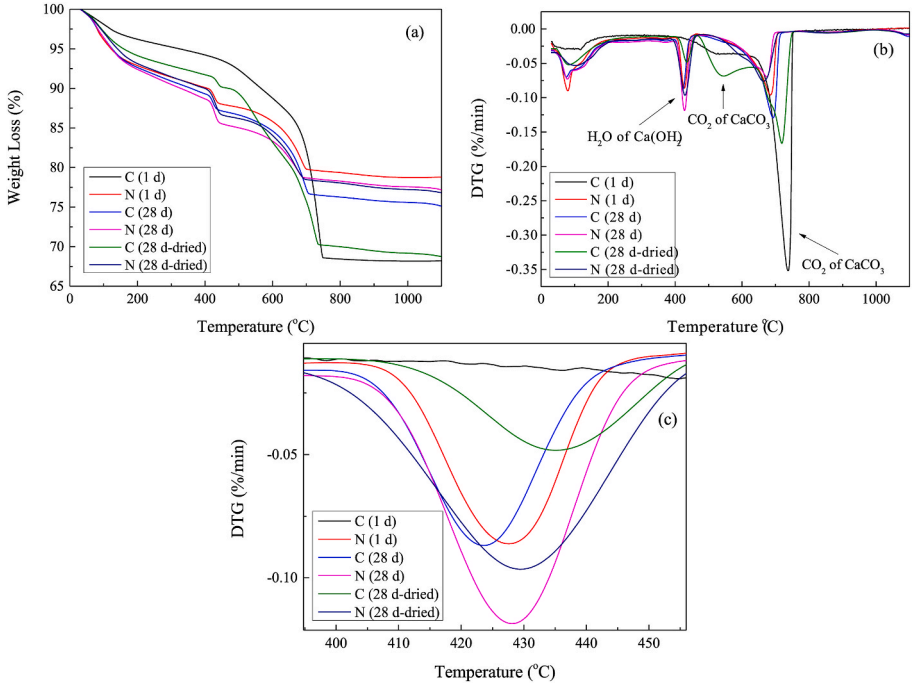

Fig. 12. (a) TG, (b) DTG, and (c) enlarged DTG curves of carbonated and non-carbonated cement pastes treated at the hydration time of 1 d, 28 d, and samples carbonated after 5 days of 50 °C-drying at hydration age of 28 d.

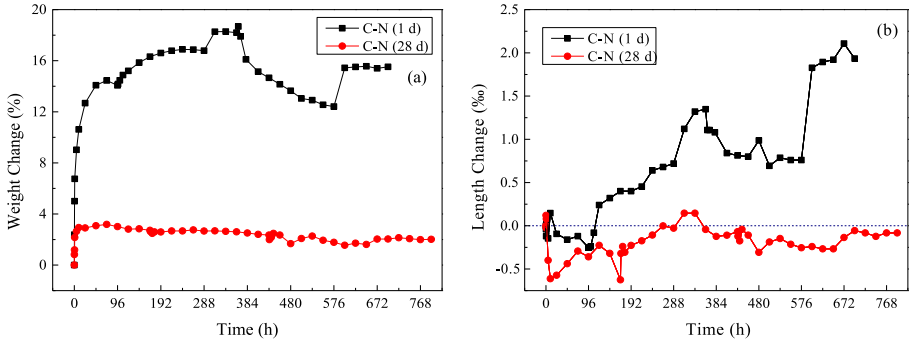

Fig. 13. Carbonation-induced (a) weight and (b) length changes of disc samples carbonated at hydration time of 1 d and 28 d.

water behavior as a whole hereafter) during and post-carbonation is important for understanding the carbonation and its influence on properties of cement pastes. To investigate the water behavior, the mass of $CaCO_3$, $Ca(OH)_2$, H_2O, and other parameters are calculated according to the results of weight monitoring, TGA, and Eqs. (4)–(6). The results are listed in Table 3.

$$\Delta m_n(A) = |m_{Cn}(A) - m_{Nn}(A)| \quad (4)$$

$$m_{theo}(H_2O) = \Delta m\left(Ca(OH)_2\right) / 74 \times 18 \quad (5)$$

$$m_{theo}(CaCO_3) = \Delta m\left(Ca(OH)_2\right) / 74 \times 100 \quad (6)$$

where n represents the hydration time of the tested samples (1 d or 28 d), A refers to $CaCO_3$, $Ca(OH)_2$, or water loss after reaction, m_{theo} means the theoretical amount of H_2O or $CaCO_3$ which could be generated by the difference in the mass of $Ca(OH)_2$ between group N and C.

As shown in Table 3, the mass of theoretical $CaCO_3$ (m_{theo} ($CaCO_3$)) is lower than the difference mass of $CaCO_3$ between group C and N (Δm ($CaCO_3$)) although the hydration degrees of group N are higher than those of group C. This indicates that in addition to $Ca(OH)_2$, there are other substances carbonated, which are mainly C–S–H gels and clinker minerals. The difference between m_{theo} ($CaCO_3$) and Δm ($CaCO_3$) of samples carbonated at 28 d is lower than that of samples carbonated at 1 d, which indicates that with the increase of hydration degree, capabilities of carbonation resistance of other carbonation reactants, e.g. C–S–H gels, are enhanced. This is consistent with [19,48] where $Ca(OH)_2$ is believed to help in limiting C–S–H decalcification or act as a buffer against carbonation of other phases. As discussed in 3.1, the carbonation product, i.e. silica-alumina gel, can be reacted in the presence of Ca ($OH)_2$. As a result, there is an equilibrium between the carbonation and the third reaction.

According to the absorptions of CO_2 from TGA and Fig. 6, the absorptions of CO_2 as a function of time are shown in Fig. 14, where the exponential relationships between weight change and time are kept and multiplied by coefficients of 1.30 ($\Delta m_1(CaCO_3) \times 0.44/13.72 \times 100$) and 1.21 ($\Delta m_{28}(CaCO_3) \times 0.44/2.91 \times 100$) for 1 d and 28 d,

Table 3
Parameters calculated according to the results of weight monitoring and TGA (Unit: g/g of starting weight of sample).

Group	C1	N1	C28	N28
m ($CaCO_3$) from TGA	0.53495	0.12990	0.18108	0.10128
m ($Ca(OH)_2$) from TGA	0	0.05738	0.05804	0.09002
m (Weight change after reaction)	0.12606	−0.01460	0.05425	0.02702
Δm ($CaCO_3$)	0.40505		0.07980	
Δm ($Ca(OH)_2$)	0.05738		0.03198	
m (Water loss after reaction)	0.10931	0.07175	0.02542	0.01755
Δm (Water loss after reaction)	0.03756		0.00788	
m_{theo} (H_2O)	–	0.01396	–	0.00778
m_{theo} ($CaCO_3$)	–	0.07754	–	0.04322

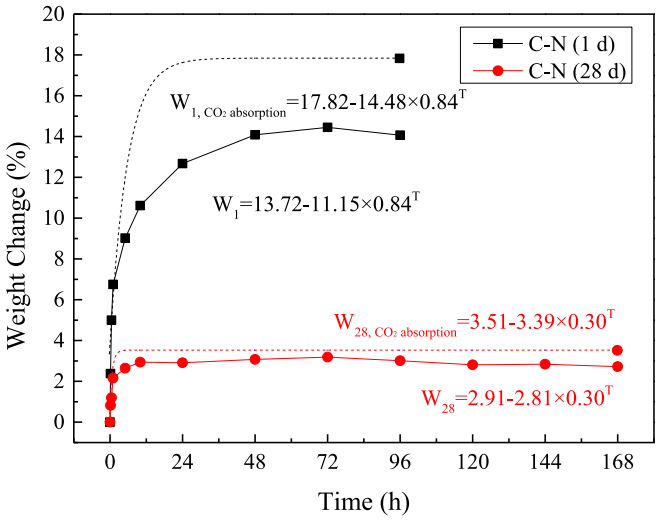

Fig. 14. Weight changes and simulative CO_2 absorption of samples carbonated at hydration time of 1 d and 28 d as a function of time.

respectively. It can be seen from Fig. 14 that carbonation induces the release of H_2O. One of the origins of the released H_2O is the carbonation of $Ca(OH)_2$ as it generates free H_2O. Whether the carbonation of C–S–H gels generates free H_2O can be verified as follows.

There are three main factors that may influence the water behavior during carbonation, which are carbonation of $Ca(OH)_2$, carbonation of C–S–H gels, and changes of pore structures. It is known that the carbonation of $Ca(OH)_2$ releases free H_2O.

For samples carbonated at 1 d, the mass of theoretical H_2O (m_{theo} (H_2O)) is lower than the difference mass of water loss after the reaction between group C and N (Δm (Water loss after reaction)), although the hydration degree of group N is higher than group C. It demonstrates H_2O may be released from pores or/and C–S–H gels.

For samples carbonated at 28 d, the m_{theo} (H_2O) is very close to Δm (Water loss after reaction). As known from Fig. 13, carbonation has little influence on the drying behavior for samples carbonated at 28 d. Therefore, it is concluded that the carbonation of C–S–H gels may not generate free H_2O. This result is consistent with [18,49]. In conclusion, during carbonation, water may be released as the carbonation of Ca ($OH)_2$ and the change of pore structures, but little released by the carbonation of C–S–H gels. And this may be one of the reason that water loss decreases when the duration of pre-carbonation hydration is prolonged [35,50].

3.6. New insight into mechanism of carbonation shrinkage

Carbonation shrinkage is possibly a potential crack risk to concrete,

particularly in accelerated carbonation. Expansion is commonly observed when the material is adsorbing substances externally. However, in the case of carbonation of cement pastes, shrinkage, instead of swelling, is always observed [19,51,52].

From the perspective of materials, $Ca(OH)_2$ is carbonated to generate $CaCO_3$, with a volume increase of about 11–14% [53]. The volume of C–S–H gels decreases after carbonation as decalcification and polymerization [6,51,54]. By using thermodynamic modeling, the solid volume of OPC paste increases at first and then decreases after consumption of $Ca(OH)_2$ with the increase of CO_2 absorption [7]. This is based on the assumption that $Ca(OH)_2$ is carbonated prior to C–S–H gels. However, the simultaneous carbonation of $Ca(OH)_2$ and C–S–H gels in cement pastes has been detected experimentally [7,55].

From the perspective of structures, it is generally believed that $CaCO_3$ mainly grows in pores and on the surfaces of existing hydration products and aggregates [18]. After carbonation, the morphology of fibrils C–S–H gels can be retained, while the inner products become porous [39]. According to the positions of $CaCO_3$ generation and changes of reaction products, an illustration of the carbonation of cement paste is proposed as shown in Fig. 15. It can be seen that carbonation of $Ca(OH)_2$ can hardly lead to a volume increase of cement paste as $CaCO_3$ mainly generates in capillary pores. Instead, cement pastes may become denser and pore structures may be refined as the carbonation of $Ca(OH)_2$. However, with the decalcification and polymerization of C–S–H gels, the inner products develop porosity, which could induce shrinkage. This agrees with the findings that the contribution of inner product C–S–H to carbonation shrinkage appears to be significant [17,23]. Carbonation shrinkage is not as considerable as other shrinkage in cement paste. However, as carbonation occurs layer by layer which develops deformation gradients, the risk of crack increases consequently.

It can also be illustrated in Fig. 15 that carbonation can lead to the redistribution of substances. The calcium in solid phases dissolves in the pore solution and reacts with CO_3^{2-} to precipitate $CaCO_3$. As a result, calcium migrates from C–S–H gels to pores. Pores are refined, while C–S–H gels become porous. Therefore, carbonation could enhance [2,9] and also degrade [49] the mechanical properties of cement pastes, which depends on the cement type and the carbonation degree.

The possibility of carbonation products generated in gel pores is considered. CO_3^{2-} ion can enter the interlayer of C–S–H gels [21]. Ca atoms are located with three statuses in C–S–H gels: Ca in main chain, Ca for charge balance (Si–OH), and Ca–OH [51,56]. It is observed that there is amorphous $CaCO_3$ in the sample carbonated at 1 d. Meanwhile, the peak temperature of calcite in 1 d carbonated sample is the highest among all samples (Fig. 12(b)). Therefore, it is deduced that the amorphous $CaCO_3$ is the combination of CO_3^{2-} ion and Ca–OH in the interlayer. This combination cannot deposit as crystal but exists as amorphous state.

This phenomenon also occurs in dried carbonated samples, which can be seen from XRD and TGA results of samples carbonated after drying as shown in Figs. 11 and 12, respectively, and from the calculated results from Fig. 12 as listed in Table 2. It can be seen that amorphous $CaCO_3$ exists in sample carbonated after 28 d-hydration and 5 d-drying, with lower decomposition temperatures than crystalline $CaCO_3$. Meanwhile, calcite, aragonite, and vaterite are all detected as shown in Fig. 11. Given that there is limited free water in capillary pores, CO_2 gets into interlayer pores, reacts with interlayer Ca^{2+}, and then precipitates as amorphous $CaCO_3$. Also, given limited free water, aragonite and vaterite can hardly evolve to calcite through dissolution-reprecipitation [57].

The corresponding length change of Fig. 5(a) could be noticed, as shown in Fig. 5(b), where the samples are carbonated with limited free water. It can be seen from Fig. 5(b) that the carbonation-induced shrinkage is about 3.5‰, which is much higher than those of samples carbonated at hydration age of 1 d and 28 d as shown in Fig. 13(b). Suppose that the main carbonated substances in cement pastes are $Ca(OH)_2$ and C–S–H gels. According to Eq. (7),

$$\frac{\text{reacted C}-\text{S}-\text{H}}{\text{reacted } Ca(OH)_2}=\frac{m_C(CaCO_3)-m_N(CaCO_3)-\left[m_N(Ca(OH)_2)-m_c(Ca(OH)_2)\right]/74\times 100}{\left[m_N(Ca(OH)_2)-m_c(Ca(OH)_2)\right]/74\times 100} \tag{7}$$

The ratio of reacted C–S–H gels to reacted $Ca(OH)_2$ in dried 28 d sample is about 2.46. This value is about 0.85 for the sample carbonated at 28 d with sufficient moisture supplied. This indicates that more C–S–H gels are carbonated in dried sample, as a consequence of the restriction of the third reaction through drying. Meanwhile, greater shrinkage is manifested (Fig. 5(b)). It is suggested that the hydration product calcium (alumino) silicate hydrates (C-(A-)S–H) is easier to collapse and redistribute upon drying as the structural incorporation of alkali cations in C-(A-)S–H reduces the stacking regularity of C-(A-)S–H layer [58]. Similarly, the incorporation of anions such as carbonate ions can also lead to the reduction in layer spacing of layered double hydroxides [59,60]. Therefore, it is speculated that the entrance of CO_3^{2-} ions into the interlayer of C–S–H gels makes the C–S–H gels easy to collapse upon drying, in other word, drying can increase carbonation shrinkage of cement pastes.

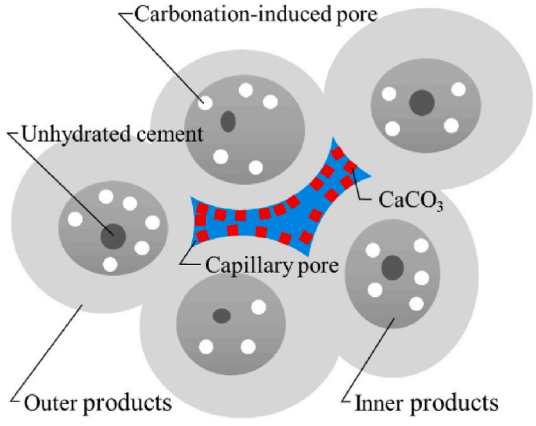

Fig. 15. Illustration of carbonation of cement paste.

4. Conclusion

The CO_2 uptake capacity of hardened cement pastes decreases dramatically with the increase of hydration time at the very beginning days of hydration, and goes relatively stable after hydrating 28 d. Two reasons for this finding are: i) The carbonation product, silica-alumina gel, could act as a reactive pozzolanic material to generate C–S–H gel through the third reaction in the presence of $Ca(OH)_2$. Hence, there is an equilibrium between the carbonation and the third reaction. The reaction moves to the later when the hydration time is prolonged enough as $Ca(OH)_2$ increases. ii) Carbonation is hindered as hydration proceeding with refined pore structures causing the difficulty of contact between carbonation reactants.

With sufficient CO_2 and moisture supplied, carbonation of disc sample occurs at a fast rate. The weight changes of 90% to equilibriums can be reached within 1 d. In this circumstance, carbonation is mainly controlled by precipitation. Calcium carbonate precipitates by the way of heterogeneous nucleation and one-dimensional growth.

A clearer partition method of carbonation zone is proposed, in which the carbonation zone is divided into 5 parts, i.e. full carbonation zone, carbonation stopped zone, carbonating zone, local diffusion zone, and non-carbonated zone. The first two belong to the carbonated zone, which is mainly controlled by diffusion. Carbonating zone and local diffusion zone belong to the partially-carbonated zone, which is mainly controlled by reaction and defect.

Carbonation reduces drying shrinkage especially for cement pastes with early ages. The influence of carbonation starts from 1 d on drying and drying shrinkage behaviors is much significant than that starts from 28 d.

Carbonation is a water release process. During carbonation, water can be released as the carbonation of $Ca(OH)_2$ and the change of pore structures, by contrast, the carbonation of C–S–H gels generates little free water.

Carbonation can lead to the redistribution of substances. Calcium migrates from C–S–H gels to pores which causes decalcification of C–S–H gels. Pores are refined, while C–S–H gels become porous, therefore, carbonation shrinkage is induced. Drying can increase carbonation shrinkage of cement pastes.

CRediT authorship contribution statement

Yaowen Xu: Conceptualization, Methodology, Formal analysis, Investigation, Writing – original draft. **Xuhui Liang:** Formal analysis, Writing – review & editing. **Chaojun Wan:** Conceptualization, Writing – review & editing, Supervision, Project administration, Funding acquisition. **Hongyu Yang:** Writing – review & editing, Supervision. **Xiaming Feng:** Writing – review & editing, Supervision.

Declaration of competing interest

The authors declare that they have no known competing financial interests or personal relationships that could have appeared to influence the work reported in this paper

Data availability

Data will be made available on request.

Acknowledgments

All authors would like to acknowledge the financial support of the National Natural Science Foundation of China [grant number 51972036].

References

[1] S.Y. Pan, T.C. Ling, A.H.A. Park, P.C. Chiang, An overview: reaction mechanisms and modelling of CO_2 utilization via mineralization, Aerosol Air Qual. Res. 18 (2018) 829–848, https://doi.org/10.4209/aaqr.2018.03.0093.

[2] V. Rostami, Y. Shao, A.J. Boyd, Carbonation curing versus steam curing for precast concrete production, J. Mater. Civ. Eng. 24 (2012) 1221–1229, https://doi.org/10.1061/(asce)mt.1943-5533.0000462.

[3] M. Liu, S. Hong, Y. Wang, J. Zhang, D. Hou, B. Dong, Compositions and microstructures of hardened cement paste with carbonation curing and further water curing, Construct. Build. Mater. 267 (2021), 121724, https://doi.org/10.1016/j.conbuildmat.2020.121724.

[4] E. Drouet, S. Poyet, P. Le Bescop, J.M. Torrenti, X. Bourbon, Carbonation of hardened cement pastes: influence of temperature, Cement Concr. Res. 115 (2019) 445–459, https://doi.org/10.1016/j.cemconres.2018.09.019.

[5] K. De Weerdt, G. Plusquellec, A. Belda Revert, M.R. Geiker, B. Lothenbach, Effect of carbonation on the pore solution of mortar, Cement Concr. Res. 118 (2019) 38–56, https://doi.org/10.1016/j.cemconres.2019.02.004.

[6] M. Auroy, S. Poyet, P. Le Bescop, J.M. Torrenti, T. Charpentier, M. Moskura, X. Bourbon, Comparison between natural and accelerated carbonation (3% CO_2): impact on mineralogy, microstructure, water retention and cracking, Cement Concr. Res. 109 (2018) 64–80, https://doi.org/10.1016/j.cemconres.2018.04.012.

[7] V. Shah, K. Scrivener, B. Bhattacharjee, S. Bishnoi, Changes in microstructure characteristics of cement paste on carbonation, Cement Concr. Res. 109 (2018) 184–197, https://doi.org/10.1016/j.cemconres.2018.04.016.

[8] B. Lu, S. Drissi, J. Liu, X. Hu, B. Song, C. Shi, Effect of temperature on CO_2 curing, compressive strength and microstructure of cement paste, Cement Concr. Res. 157 (2022), 106827, https://doi.org/10.1016/j.cemconres.2022.106827.

[9] X. Xian, D. Zhang, H. Lin, Y. Shao, Ambient pressure carbonation curing of reinforced concrete for CO_2 utilization and corrosion resistance, J. CO_2 Util. 56 (2022), 101861, https://doi.org/10.1016/j.jcou.2021.101861.

[10] Z. He, Y. Jia, S. Wang, M. Mahoutian, Y. Shao, Maximizing CO_2 sequestration in cement-bonded fiberboards through carbonation curing, Construct. Build. Mater. 213 (2019) 51–60, https://doi.org/10.1016/j.conbuildmat.2019.04.042.

[11] N. Lippiatt, T.C. Ling, S. Eggermont, Combining hydration and carbonation of cement using super-saturated aqueous CO_2 solution, Construct. Build. Mater. 229 (2019), 116825, https://doi.org/10.1016/j.conbuildmat.2019.116825.

[12] X. Li, T.C. Ling, Instant CO_2 curing for dry-mix pressed cement pastes: consideration of CO_2 concentrations coupled with further water curing, J. CO_2 Util. 38 (2020) 348–354, https://doi.org/10.1016/j.jcou.2020.02.012.

[13] T. Chen, M. Bai, X. Gao, Carbonation curing of cement mortars incorporating carbonated fly ash for performance improvement and CO_2 sequestration, J. CO_2 Util. 51 (2021), 101633, https://doi.org/10.1016/j.jcou.2021.101633.

[14] T. Chen, X. Gao, L. Qin, Mathematical modeling of accelerated carbonation curing of Portland cement paste at early age, Cement Concr. Res. 120 (2019) 187–197, https://doi.org/10.1016/j.cemconres.2019.03.025.

[15] B. Šavija, M. Luković, Carbonation of cement paste: understanding, challenges, and opportunities, Construct. Build. Mater. 117 (2016) 285–301, https://doi.org/10.1016/j.conbuildmat.2016.04.138.

[16] C. Liang, B. Pan, Z. Ma, Z. He, Z. Duan, Utilization of CO_2 curing to enhance the properties of recycled aggregate and prepared concrete : a review, Cem. Concr. Compos. 105 (2020), 103446, https://doi.org/10.1016/j.cemconcomp.2019.103446.

[17] G.W. Groves, D.I. Rodway, I.G. Richardson, The carbonation of hardened cement pastes, Adv. Cement Res. 3 (1990) 117–125, https://doi.org/10.1680/adcr.1990.3.11.117.

[18] A. Morandeau, M. Thiery, P. Dangla, Investigation of the carbonation mechanism of CH and C-S-H in terms of kinetics, microstructure changes and moisture properties, Cem, Concr. Res. 56 (2014) 153–170, https://doi.org/10.1016/j.cemconres.2013.11.015.

[19] E. Kangni-Foli, S. Poyet, P. Le Bescop, T. Charpentier, F. Bernachy-Barbe, A. Dauzeres, E. L'Hôpital, J.B. d'Espinose de Lacaillerie, Carbonation of model cement pastes: the mineralogical origin of microstructural changes and shrinkage, Cement Concr. Res. 144 (2021), https://doi.org/10.1016/j.cemconres.2021.106446.

[20] M. Auroy, S. Poyet, P. Le Bescop, J.M. Torrenti, T. Charpentier, M. Moskura, X. Bourbon, Impact of carbonation on unsaturated water transport properties of cement-based materials, Cement Concr. Res. 74 (2015) 44–58, https://doi.org/10.1016/j.cemconres.2015.04.002.

[21] Y. Li, W. Liu, F. Xing, S. Wang, L. Tang, S. Lin, Z. Dong, Carbonation of the synthetic calcium silicate hydrate (C-S-H) under different concentrations of CO_2: chemical phases analysis and kinetics, J. CO_2 Util. 35 (2020) 303–313, https://doi.org/10.1016/j.jcou.2019.10.001.

[22] L. Liu, X. Wang, H. Chen, C. Wan, Microstructure-based modelling of drying shrinkage and microcracking of cement paste at high relative humidity, Construct. Build. Mater. 126 (2016) 410–425, https://doi.org/10.1016/j.conbuildmat.2016.09.066.

[23] J.J. Chen, J.J. Thomas, H.M. Jennings, Decalcification shrinkage of cement paste, Cement Concr. Res. 36 (2006) 801–809, https://doi.org/10.1016/j.cemconres.2005.11.003.

[24] K. Wan, Q. Xu, Y. Wang, G. Pan, 3D spatial distribution of the calcium carbonate caused by carbonation of cement paste, Cem. Concr. Compos. 45 (2014) 255–263, https://doi.org/10.1016/j.cemconcomp.2013.10.011.

[25] J. Han, W. Sun, G. Pan, W. Caihui, Monitoring the evolution of accelerated carbonation of hardened cement pastes by X-ray computed tomography, J. Mater. Civ. Eng. 25 (2013) 347–354, https://doi.org/10.1061/(asce)mt.1943-5533.0000610.

[26] J. Wang, H. Xu, D. Xu, P. Du, Z. Zhou, L. Yuan, X. Cheng, Accelerated carbonation of hardened cement pastes: influence of porosity, Construct. Build. Mater. 225 (2019) 159–169, https://doi.org/10.1016/j.conbuildmat.2019.07.088.

[27] X. Xian, Y. Shao, Microstructure of cement paste subject to ambient pressure carbonation curing, Construct. Build. Mater. 296 (2021), 123652, https://doi.org/10.1016/j.conbuildmat.2021.123652.

[28] Q. Shen, G. Pan, B. Bao, Influence of CSH carbonation on the porosity of cement paste, Mag. Concr. Res. 68 (2016) 504–514, https://doi.org/10.1680/jmacr.15.00286.

[29] GB8076-2008, Concrete Admixtures, China National Standard, China, 2008.

[30] K. Scrivener, R. Snellings, B. Lothenbach, A Practical Guide to Microstructural Analysis of Cementitious Materials, 2018, https://doi.org/10.1201/b19074.

[31] M. Zajac, J. Skibsted, P. Durdzinski, F. Bullerjahn, J. Skocek, M. Ben Haha, Kinetics of enforced carbonation of cement paste, Cement Concr. Res. 131 (2020), 106013, https://doi.org/10.1016/j.cemconres.2020.106013.

[32] M. Zajac, A. Lechevallier, P. Durdzinski, F. Bullerjahn, J. Skibsted, M. Ben, CO_2 mineralisation of Portland cement : towards understanding the mechanisms of

enforced carbonation, J. CO_2 Util. 38 (2020) 398–415, https://doi.org/10.1016/j.jcou.2020.02.015.
[33] M. Zajac, J. Skocek, P. Durdzinski, F. Bullerjahn, J. Skibsted, M. Ben Haha, Effect of carbonated cement paste on composite cement hydration and performance, Cement Concr. Res. 134 (2020), 106090, https://doi.org/10.1016/j.cemconres.2020.106090.
[34] O. Linderoth, L. Wadsö, D. Jansen, Long-term cement hydration studies with isothermal calorimetry, Cement Concr. Res. 141 (2021), https://doi.org/10.1016/j.cemconres.2020.106344.
[35] D. Zhang, X. Cai, B. Jaworska, Effect of pre-carbonation hydration on long-term hydration of carbonation-cured cement-based materials, Construct. Build. Mater. 231 (2020), 117122, https://doi.org/10.1016/j.conbuildmat.2019.117122.
[36] M. Avrami, Kinetics of phase change. I: general theory, J. Chem. Phys. 7 (1939) 1103–1112, https://doi.org/10.1063/1.1750380.
[37] M. Avrami, Kinetics of phase change. II Transformation-time relations for random distribution of nuclei, J. Chem. Phys. 8 (1940) 212–224, https://doi.org/10.1063/1.1750631.
[38] J.J. Thomas, J.J. Biernacki, J.W. Bullard, S. Bishnoi, J.S. Dolado, G.W. Scherer, A. Luttge, Modeling and simulation of cement hydration kinetics and microstructure development, Cement Concr. Res. 41 (2011) 1257–1278, https://doi.org/10.1016/j.cemconres.2010.10.004.
[39] G.W. Groves, A. Brough, I.G. Richardson, C.M. Dobson, Progressive changes in the structure of hardened C_3S cement pastes due to carbonation, J. Am. Ceram. Soc. 74 (1991) 2891–2896, https://doi.org/10.1111/j.1151-2916.1991.tb06859.x.
[40] A. Vollpracht, B. Lothenbach, R. Snellings, J. Haufe, The pore solution of blended cements: a review, Mater. Struct. Constr. 49 (2016) 3341–3367, https://doi.org/10.1617/s11527-015-0724-1.
[41] Y.S. Ji, M. Wu, B. Ding, F. Liu, F. Gao, The experimental investigation of width of semi-carbonation zone in carbonated concrete, Construct. Build. Mater. 65 (2014) 67–75, https://doi.org/10.1016/j.conbuildmat.2014.04.095.
[42] K. Tuutti, Corrosion of Steel in Concrete, Swedish Cement and Concrete Research Institute, Stockholm, 1982.
[43] GB/T50082-2009, Standard for Test Methods of Long-Term Performance and Durability of Ordinary Concrete, Ministry of Housing and Urban-Rural Development of the People's Republic of China, Beijing, 2009.
[44] EN12390-12, Testing Hardened Concrete - Part 12: Determination of the Carbonation Resistance of Concrete - Accelerated Carbonation Method, European committee for standardization, Brussels, 2020.
[45] V. Dutzer, W. Dridi, S. Poyet, P. Le Bescop, X. Bourbon, The link between gas diffusion and carbonation in hardened cement pastes, Cement Concr. Res. 123 (2019), 105795, https://doi.org/10.1016/j.cemconres.2019.105795.
[46] J.S. Kim, K.S. Youm, J.H. Lim, T.S. Han, Effect of carbonation on cement paste microstructure characterized by micro-computed tomography, Construct. Build. Mater. 263 (2020), 120079, https://doi.org/10.1016/j.conbuildmat.2020.120079.
[47] M.C. Garci Juenger, H.M. Jennings, Examining the relationship between the microstructure of calcium silicate hydrate and drying shrinkage of cement pastes, Cement Concr. Res. 32 (2002) 289–296, https://doi.org/10.1016/S0008-8846(01)00673-1.
[48] J. Herterich, I. Richardson, F. Moro, M. Marchi, L. Black, Microstructure and phase assemblage of low-clinker cements during the early stages of carbonation, Cement Concr. Res. 152 (2022), 106643, https://doi.org/10.1016/j.cemconres.2021.106643.
[49] X. Zha, J. Ning, M. Saafi, L. Dong, J.B.M. Dassekpo, J. Ye, Effect of supercritical carbonation on the strength and heavy metal retention of cement-solidified fly ash, Cement Concr. Res. 120 (2019) 36–45, https://doi.org/10.1016/j.cemconres.2019.03.005.
[50] D. Zhang, V.C. Li, B.R. Ellis, Optimal pre-hydration age for CO_2 sequestration through portland cement carbonation, ACS Sustain. Chem. Eng. 6 (2018) 15976–15981, https://doi.org/10.1021/acssuschemeng.8b03699.
[51] F. Matsushita, Y. Aono, S. Shibata, Calcium silicate structure and carbonation shrinkage of a tobermorite-based material, Cement Concr. Res. 34 (2004) 1251–1257, https://doi.org/10.1016/j.cemconres.2003.12.016.
[52] P.H.R. Borges, J.O. Costa, N.B. Milestone, C.J. Lynsdale, R.E. Streatfield, Carbonation of CH and C-S-H in composite cement pastes containing high amounts of BFS, Cement Concr. Res. 40 (2010) 284–292, https://doi.org/10.1016/j.cemconres.2009.10.020.
[53] B. Lagerblad, Carbon Dioxide Uptake during Concrete Life Cycle - State of the Art, 2005.
[54] B. Li, Z. Sun, K. Hu, J. Yang, Influence of carbonation on the volume change of hardened cement pastes, Construct. Build. Mater. 260 (2020), 119709, https://doi.org/10.1016/j.conbuildmat.2020.119709.
[55] M. Castellote, C. Andrade, X. Turrillas, J. Campo, G.J. Cuello, Accelerated carbonation of cement pastes in situ monitored by neutron diffraction, Cem, Concr. Res. 38 (2008) 1365–1373, https://doi.org/10.1016/j.cemconres.2008.07.002.
[56] J.J. Chen, J.J. Thomas, H.F.W. Taylor, H.M. Jennings, Solubility and structure of calcium silicate hydrate, Cement Concr. Res. 34 (2004) 1499–1519, https://doi.org/10.1016/j.cemconres.2004.04.034.
[57] T. Ogino, T. Suzuki, K. Sawada, The formation and transformation mechanism of calcium carbonate in water, Geochem. Cosmochim. Acta 51 (1987) 2757–2767, https://doi.org/10.1016/0016-7037(87)90155-4.
[58] H. Ye, A. Radlinska, Shrinkage mechanisms of alkali-activated slag, Cement Concr. Res. 88 (2016) 126–135, https://doi.org/10.1016/j.cemconres.2016.07.001.
[59] I.G. Richardson, The importance of proper crystal-chemical and geometrical reasoning demonstrated using layered single and double hydroxides, Acta Crystallogr. Sect. B Struct. Sci. Cryst. Eng. Mater. 69 (2013) 150–162, https://doi.org/10.1107/S205251921300376X.
[60] I.G. Richardson, Zn- and Co-based layered double hydroxides: prediction of the a parameter from the fraction of trivalent cations and vice versa, Acta Crystallogr. Sect. B Struct. Sci. Cryst. Eng. Mater. 69 (2013) 414–417, https://doi.org/10.1107/S2052519213017545.